PHYSICAL REVIEW A

GENERAL PHYSICS

THIRD SERIES, VOLUME 37, NUMBER 2 JANUARY 15, 1988

Finite basis sets for the Dirac equation constructed from *B* splines

W. R. Johnson, S. A. Blundell, and J. Sapirstein
Department of Physics, University of Notre Dame, Notre Dame, Indiana 46556
(Received 31 July 1987)

A procedure is given for constructing basis sets for the radial Dirac equation from *B* splines. The resulting basis sets, which include negative-energy states in a natural way, permit the accurate evaluation of the multiple sums over intermediate states occurring in relativistic many-body calculations. Illustrations are given for the Coulomb-field Dirac equation and tests of the resulting basis sets are described. As an application, relativistic corrections to the second-order correlation energy in helium are calculated. Another application is given to determine the spectrum of thallium (where finite–nuclear-size effects are important) in a model potential. Construction of *B*-spline basis sets for the Dirac-Hartree-Fock equations is described and the resulting basis sets are applied to study the cesium spectrum.

INTRODUCTION

Relativistic many-body perturbation theory applied to calculations of properties of heavy atoms starting from the radial Dirac equation often leads to sums over intermediate states that are difficult to evaluate accurately. Part of the difficulty stems from the fact that the spectrum of the Dirac equation is complicated; it consists of an infinite set of bound states, a positive-energy continuum, and a negative-energy continuum.

One method used to evaluate sums over intermediate states is to saturate the contributions from the discrete part of the spectrum and to add integrals over the continuous parts of the spectrum. The principal source of difficulty with this direct approach is that one must account for the remainders of the sums and integrals using inherently inaccurate extrapolation techniques. Although the direct method is difficult to apply with high accuracy, it has been used successfully to evaluate sums occurring in nonrelativistic[1] and in relativistic[2] many-body perturbation theory.

An alternative that is often used to evaluate single sums is to convert the sums into integrals over the solutions to inhomogeneous differential equations using the Sternheimer[3] or Dalgarno-Lewis[4] method. In the relativistic case the differential equations are inhomogeneous Dirac equations that can be solved with high accuracy using standard finite-difference methods; the integrals can also be evaluated accurately using standard numerical techniques. This is the simplest method to obtain highly accurate values for sums over a single set of intermediate states.

Double sums over intermediate states such as those occurring in the evaluation of the second-order corrections to energies can be converted into double integrals over solutions to partial differential equations in two radial variables. The resulting equations (the pair equations) are routinely solved in the nonrelativistic case.[5–7] Because of the extra spatial dimension, it is relatively time consuming to solve a pair equation and obtain the corresponding pair function with the same high accuracy as is typically achieved in solving one-dimensional differential equations. Furthermore, in the relativistic case there are usually restrictions on the range of the summation indices, leading to the appearance of projection operators in the inhomogeneous term of the pair equation. Although projection operators for the Dirac equation in a potential are not known in closed analytic form they can be obtained by an iteration scheme. An application of the relativistic pair equation to the helium isoelectronic sequence has recently been made by Lindroth.[8]

To facilitate the accurate evaluation of intermediate state sums, especially multiple sums, we introduce a finite basis for the radial Dirac equation, and replace sums over states of the Dirac equation in a potential by sums over the finite basis set. Since the resulting sums are finite, there are no remainders to evaluate. Furthermore, in the relativistic case, projection operators may be introduced directly by restricting the range of the summation indices. Finite basis sets for the Dirac equation have received a great deal of attention during the past few years, and a number of successful attempts have been made to apply finite basis techniques to problems in relativistic quantum mechanics.[9–11]

We are particularly interested in applying the finite

basis states to analyze relativistic pair functions. From nonrelativistic studies it is well established that pair functions are compact; the pair functions vanish exponentially outside atomic dimensions. For our purposes it is therefore possible to constrain the basis functions used to approximate the pair functions to a cavity of finite radius R. (In practice we choose $R=40$ a.u. for calculations of alkali-metal atom pair functions, and increase R by a factor of 1.5 to determine the sensitivity to the cavity radius.)

If we let $P_{nl}(r)$ denote a nonrelativistic radial wave function, then the cavity constraint is imposed using the boundary condition

$$P_{nl}(R)=0 \ . \tag{1}$$

In the relativistic case the generalization of this condition is given by the Massachusetts Institute of Technology (MIT) bag-model boundary condition[12]

$$P_{n\kappa}(R)=Q_{n\kappa}(R) \ , \tag{2}$$

where $P_{n\kappa}(r)$ and $Q_{n\kappa}(r)$ are the large and small component radial wave functions, respectively. The relative phase in Eq. (2) depends on the phase convention used in the angular separation of the single-particle Dirac wave function: in the following paragraphs we adopt the convention

$$\psi_{n\kappa m}(\mathbf{r})=\frac{1}{r}\begin{bmatrix} iP_{n\kappa}(r)\chi_{\kappa m}(\hat{r}) \\ Q_{n\kappa}(r)\chi_{-\kappa m}(\hat{r}) \end{bmatrix} \ , \tag{3}$$

where $\chi_{\kappa m}(\hat{r})$ is an ls coupled spherical spinor. We use the MIT–bag-model boundary conditions in order to avoid problems with the "Klein paradox" that arise in the relativistic case when one attempts to confine a particle to a cavity using an infinite potential barrier at $r=R$.[13] Imposing the MIT–bag-model boundary condition modifies the spectrum of the Dirac equation. The modified spectrum consists of two infinite discrete spectra, one with positive energies and one with negative energies. The positive-energy branch of the cavity spectrum contains the terms that belonged to the bound-state spectrum as well as terms that belonged to the positive-energy continuum of the unmodified spectrum. The low-lying positive-energy states in the cavity spectrum agree very closely with the low-lying states in the original discrete spectrum, but as the principal quantum number increases the effects of the cavity modify the spectrum more and more strongly. It is the discrete finite-cavity spectrum, not the original spectrum of the Dirac equation, that we approximate by a finite basis set.

One way to understand our particular finite-basis-set approximation is to imagine that we are approximating solutions to the Dalgarno-Lewis differential equation in the one-dimensional case, or to the pair equations in the two-dimensional case. The solutions to these differential equations are smooth functions of r that vanish outside atomic dimensions. It is possible to approximate such smooth compact functions to high accuracy using piecewise polynomials. First, the radial grid from $r=0$ to $r=R$ is divided up into segments. We then introduce a family of polynomials of a fixed degree on each segment and adjust the coefficients of the resulting piecewise polynomials to fit the functions of interest as well as possible. Approximating known functions by piecewise polynomials can be done in a completely systematic way using B splines.[14]

DESCRIPTION OF THE B-SPLINE APPROXIMATION SCHEME

Our aim is to approximate solutions of the Dirac equation in a cavity of radius R with piecewise polynomials, using B splines to systematize the analysis. Following the notation of deBoor[14] we designate the endpoints of the segments on the x axis by the "knot sequence" $\{t_i\}, i=1,2,\ldots$. The B splines of order k, $B_{i,k}(x)$, on this knot sequence may be defined recursively by the relations[14]

$$B_{i,1}(x)=\begin{cases} 1, & t_i \le x < t_{i+1} \\ 0, & \text{otherwise} \end{cases} \tag{4}$$

and

$$B_{i,k}(x)=\frac{x-t_i}{t_{i+k-1}-t_i}B_{i,k-1}(x) + \frac{t_{i+k}-x}{t_{i+k}-t_{i+1}}B_{i+1,k-1}(x) \ . \tag{5}$$

It follows that $B_{i,k}(x)$ is a piecewise polynomial of degree $k-1$ that vanishes except in the interval $t_i \le x < t_{i+k}$. A software package written in FORTRAN is available[14] to generate all of the nonvanishing B splines of order k associated with the knot sequence $\{t_i\}$ using the recursion relations. As an example consider the knot sequence $t_1=t_2=t_3=0$, $t_i=(i-3)$, $i=4,\ldots,12$, and $t_{13}=t_{14}=t_{15}=10$. The endpoints 0 and 10 are associated with "multiple knots" (in this case, knots of multiplicity 2) and are calculated using limiting forms of the above recursion relations. In Fig. 1 the 12 B splines

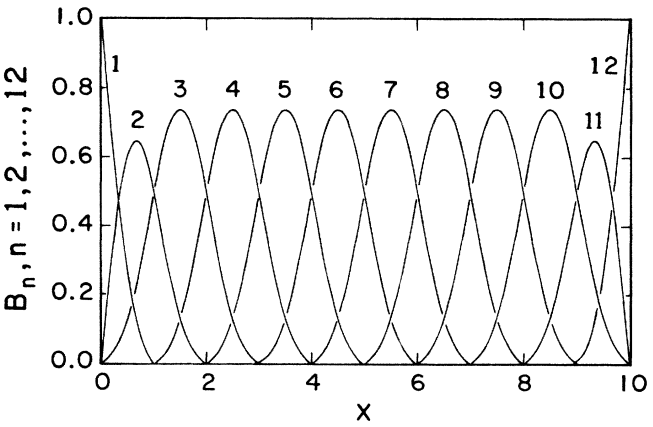

FIG. 1. The twelve B splines of order $k=3$, $B_{i,3}(x)$, for the uniform knot sequence $t_1=t_2=t_3=0$, $t_4=1, t_5=2\ldots$, $t_{12}=9$, $t_{13}=t_{14}=t_{15}=10$ are shown. At any point there are three nonvanishing functions that sum to 1. In our applications to the Dirac equation, B splines of orders 7–9 are used and the knot sequence is distributed exponentially rather than uniformly.

of order 3 associated with the knot sequence $\{t_i\}$, $i=1,15$ are shown. Each of these functions $B_{i,3}(x)$ vanishes outside the interval $t_i<x<t_{i+3}$; in the interval each function is a polynomial of degree 2. At the known boundaries between segments each function $B_{i,3}(x)$ is continuous and has a continuous first derivative. At the endpoints, which are knots of multiplicity 2, the functions $B_{1,3}(x)$ and $B_{12,3}(x)$ are discontinuous, whereas $B_{2,3}(x)$ and $B_{11,3}(x)$ have discontinuous first derivatives. It should be noticed that the sum of the nonvanishing B splines at any point is exactly 1. In this example we have shown B splines of order 3 on a uniform grid with endpoints of multiplicity 2. In our applications we use B splines of higher order; we have found that splines of orders $k=7$ and 9 are accurate enough for most of our calculations, without being too cumbersome to manipulate. The knots defining our grid have k-fold multiplicity at the endpoints $r=0$ and $r=R=40$ a.u., and are distributed exponentially rather than uniformly in the interval between the endpoints.

The set of B splines of order k on a knot sequence $\{t_i\}$ forms a complete basis for piecewise polynomials of degree $k-1$ on the intervals defined by the knot sequence. We represent the solution to the Dirac equation as linear combinations of these B splines and we work with the B spline representation of the functions, rather than with the functions themselves. The radial Dirac equation can be written

$$\begin{bmatrix} V(r) & c(d/dr-\kappa/r) \\ -c(d/dr+\kappa/r) & -2mc^2+V(r) \end{bmatrix} \begin{bmatrix} P_\kappa(r) \\ Q_\kappa(r) \end{bmatrix} = \epsilon \begin{bmatrix} P_\kappa(r) \\ Q_\kappa(r) \end{bmatrix} . \quad (6)$$

This form is slightly different from the one appearing in textbooks in that we have replaced the energy E by $\epsilon=E-mc^2$ to facilitate comparisons with nonrelativistic calculations. The negative-energy states are those with $\epsilon<-2mc^2$, whereas the positive-energy states have $\epsilon<0$ for low-lying states and $\epsilon>0$ for the higher states. One approach to approximating Eqs. (6) is to expand the equations in terms of basis functions and then demand that the resulting equations be satisfied at a suitably chosen set of *collocation points.* This approach has been successfully applied to the Dirac equations by Bottcher and Strayer.[15] Another approach, which is employed here, is to use a *Galerkin method;*[16] the equations are expressed in terms of an action principle, and the action integral is expanded in terms of basis functions. The radial Dirac equations (6) can be derived from an action principle $\delta S=0$, with

$$S=\tfrac{1}{2}\int_0^R \{cP_\kappa(r)(d/dr-\kappa/r)Q_\kappa(r)-cQ_\kappa(r)(d/dr+\kappa/r)P_\kappa(r)+V(r)[Q_\kappa(r)^2+P_\kappa(r)^2] -2mc^2Q_\kappa(r)^2\}dr-\tfrac{1}{2}\epsilon\int_0^R[P_\kappa(r)^2+Q_\kappa(r)^2]dr . \quad (7)$$

From the point of view of the variational principle, the parameter ϵ is a Lagrange multiplier introduced to ensure that the normalization constraint,

$$\int_0^R [P_\kappa(r)^2+Q_\kappa(r)^2]dr=1 , \quad (8)$$

is satisfied. The first variation of S is given by

$$\delta S=\int_0^R(\delta P_\kappa(r)[c(d/dr-\kappa/r)Q_\kappa(r)+V(r)P_\kappa(r)]-\delta Q_\kappa(r)\{c(d/dr+\kappa/r)P_\kappa(r)+[2mc^2-V(r)]Q_\kappa(r)\})dr -\epsilon\int_0^R[\delta P_\kappa(r)P_\kappa(r)+\delta Q_\kappa(r)Q_\kappa(r)]dr+\tfrac{1}{2}c[P_\kappa(r)\delta Q_k(r)-Q_\kappa(r)\delta P_\kappa(r)]_0^R . \quad (9)$$

The requirement $\delta S=0$ for variations of $P_\kappa(r)$ and $Q_\kappa(r)$ satisfying the constraints $\delta P_\kappa(0)=\delta Q_\kappa(0)=0$ and $\delta P_\kappa(R)=\delta Q_\kappa(R)=0$ leads to the radial Dirac equations written down in Eq. (6). Specific boundary conditions can be imposed on the solutions by removing the boundary constraints from the variational functions $\delta P_\kappa(r)$ and $\delta Q_\kappa(r)$ and by adding appropriate boundary terms to the action integral S. In the present case we add to S the boundary term

$$S'=\begin{cases} \frac{c}{4}[P_\kappa(R)^2-Q_\kappa(R)^2]+\frac{c}{2}P_\kappa(0)^2-\frac{c'}{2}P_\kappa(0)Q_\kappa(0) & \text{for } \kappa<0 , \quad (10a) \\ \frac{c}{4}[P_\kappa(R)^2-Q_\kappa(R)^2]+c^2P_\kappa(0)^2-\frac{c}{2}P_\kappa(0)Q_\kappa(0) & \text{for } \kappa>0 . \quad (10b) \end{cases}$$

Combining the boundary term in Eq. (9) with the terms obtained from the variation of Eqs. (10a) and (10b) lead to boundary terms given by

$$\delta(S+S')_{\text{boundary}}=\begin{cases} \frac{c}{2}[P_\kappa(R)-Q_\kappa(R)]\delta Q_\kappa(R)+\frac{c}{2}[P_\kappa(R)-Q_\kappa(R)]\delta P_\kappa(R)-cP_\kappa(0)\delta Q_\kappa(0)+cP_\kappa(0)\delta P_\kappa(0), & \kappa<0 \quad (11a) \\ \frac{c}{2}[P_\kappa(R)-Q_\kappa(R)]\delta Q_\kappa(R)+\frac{c}{2}[P_\kappa(R)-Q_\kappa(R)]\delta P_\kappa(R)-cP_\kappa(0)\delta Q_\kappa(0)+2c^2P_\kappa(0)\delta P_\kappa(0), & \kappa>0 . \quad (11b) \end{cases}$$

For variations of $P_\kappa(r)$ and $Q_\kappa(r)$, *not* subject to boundary constraints, the boundary terms in Eqs. (11a) and (11b) vanish if

$$P_\kappa(R)=Q_\kappa(R)\ , \tag{12}$$

which is just the MIT-bag-model boundary condition, and if

$$P_\kappa(0)=0\ . \tag{13}$$

The choice of the boundary terms in Eqs. (10a) and (10b) is to some extent arbitrary; the particular choice made here was found to eliminate spurious states that can occur in the spectrum for $\kappa>0$ when the Dirac equation is expanded in terms of finite basis sets.[9]

We expand the radial functions $P_\kappa(r)$ and $Q_\kappa(r)$ in terms of B splines of order k as

$$\begin{aligned} P(r)&=\sum_{i=1}^{n} p_i B_i(r)\ , \\ Q(r)&=\sum_{i=1}^{n} q_i B_i(r)\ . \end{aligned} \tag{14}$$

The subscript κ has been omitted from the functions $P_\kappa(r)$ and $Q_\kappa(r)$ and the subscript k has been omitted on the functions $B_{i,k}(x)$ for notational simplicity. Substituting these expressions into the action functional leads to a quadratic form in p_i and q_i for $S+S'$. The variational principle reduces to the following system of algebraic equations:

$$d(S+S')/dp_i=0,\quad i=1,2,\ldots,n \tag{15a}$$

and

$$d(S+S')/dq_i=0,\quad i=1,2,\ldots,n\ . \tag{15b}$$

These equations can be expressed in the form of a $2n\times 2n$ symmetric generalized eigenvalue equation

$$Av=\epsilon Bv\ , \tag{16}$$

where the $2n$ vector v is given by

$$v=(p_1,p_2,\ldots,p_n,q_1,q_2,\ldots,q_n)\ , \tag{17}$$

and where A and B are symmetric $2n\times 2n$ matrices. Specifically,

$$A=\begin{bmatrix} (V) & c[(D)-(\kappa/r)] \\ -c[(D)+(\kappa/r)] & -2mc^2(C)+(V) \end{bmatrix}+A'\ , \tag{18}$$

$$B=\begin{bmatrix} (C) & 0 \\ 0 & (C) \end{bmatrix}\ , \tag{19}$$

where the $2n\times 2n$ matrix A' is a contribution from the boundary terms

$$A'_{ij}=\begin{cases} c\delta_{i,1}\delta_{j,1}-\dfrac{c}{2}\delta_{i,1}\delta_{j,n+1}-\dfrac{c}{2}\delta_{i,n+1}\delta_{j,1} \\ +\dfrac{c}{2}\delta_{i,n}\delta_{j,n}-\dfrac{c}{2}\delta_{i,2n}\delta_{j,2n},\quad \kappa<0\ , \end{cases} \tag{20a}$$

$$A'_{ij}=\begin{cases} 2c^2\delta_{i,1}\delta_{j,1}-\dfrac{c}{2}\delta_{i,1}\delta_{j,n+1}-\dfrac{c}{2}\delta_{i,n+1}\delta_{j,1} \\ +\dfrac{c}{2}\delta_{i,n}\delta_{j,n}-\dfrac{c}{2}\delta_{i,2n}\delta_{j,2n},\quad \kappa>0\ . \end{cases} \tag{20b}$$

The $n\times n$ matrices (C), (D), (V), and (κ/r) are given by

$$(C)_{ij}=\int B_i(r)B_j(r)dr\ , \tag{21a}$$

$$(D)_{ij}=\int B_i(r)dB_j(r)/dr\ , \tag{21b}$$

$$(V)_{ij}=\int B_i(r)V(r)B_j(r)dr\ , \tag{21c}$$

$$(\kappa/r)_{ij}=\int B_i(r)\kappa/rB_j(r)dr\ . \tag{21d}$$

One important numerical point to be mentioned is that the matrices (C), (D), (V), and (κ/r) are diagonally dominant banded matrices, so that the numerical solution of the generalized eigenvalue equation (16) can be carried out with high accuracy even when the dimensions of the basis set become very large. To solve the eigenvalue problem we use subroutines from the FORTRAN EISPACK library.[17] If we let v_i^λ be the eigenvector associated with eigenvalue ϵ_λ then we find.

$$\sum_{i,j} v_i^\lambda (B)_{ij} v_j^\sigma=\delta_{\lambda\sigma}\ . \tag{22}$$

Written in terms of the approximate eigenfunctions $P^\lambda(r)$ and $Q^\lambda(r)$ this equation expresses the orthonormality conditions

$$\int [P^\lambda(r)P^\sigma(r)+Q^\lambda(r)Q^\sigma(r)]dr=\delta_{\lambda\sigma}\ . \tag{23}$$

To summarize, the symmetric generalized eigenvalue equation (16) is solved to give $2n$ eigenvalues ϵ_λ and $2n$ orthonormal eigenfunctions

$$P^\lambda(r)=\sum_{i=1}^{n} v_i^\lambda B_i(r)\ , \tag{24}$$

$$Q^\lambda(r)=\sum_{i=n+1}^{2n} v_i^\lambda B_i(r)\ . \tag{25}$$

Let us consider, as an illustration, the case of a Coulomb field with charge $Z=2$. We choose a cavity radius $R=40.0$ a.u., and examine the approximate cavity spectrum of the Dirac equation for $\kappa=-1$. We express our wave functions as linear combinations of B splines with $n=40$ and $k=7$. In Table I we list the 80 eigenvalues given by solving Eq. (16). As is seen from the table, 40 of these eigenvalues lie below $-2mc^2$, while the remaining 40 eigenvalues (the positive-energy group) grow from small negative values to large positive values. The lowest few terms of the positive-energy spectrum given in column 3, the eigenvalues of the low-lying bound states, are seen to be very close to the exact eigenvalues of the Coulomb-field Dirac equation in the absence of a cavity, given in column 5 of the table.

There are several tests of the quality of this spectrum that can be easily carried out. One test is to determine how well the Thomas-Reiche-Kuhn (TRK) sum rule is satisfied. This rule can be formulated in the relativistic case in terms of the two partial waves $\kappa=l$, and $\kappa=-l-1$ associated with orbital angular momentum l

$$\left[\frac{l}{2l+1}\sum_n \omega_{n0}|\langle\kappa=-1, n=0|r|\kappa=l, n\rangle|^2+\frac{l+1}{2l+1}\sum_n \omega_{n0}|\langle\kappa=-1, n=0|r|\kappa=-l-1, n\rangle|^2\right]=0\ , \tag{26}$$

where $\omega_{n0}=\epsilon_{n,\kappa}-\epsilon_{0,-1}$. For the nonrelativistic case the corresponding TRK sum rule is

$$\sum_n \omega_{n0}|\langle l=0, n=0|r|l,n\rangle|^2=\frac{l(l+1)+1}{2}\ . \tag{27}$$

The sum over the positive-energy states in the relativistic TRK sum rule gives a value close to the nonrelativistic expression, but this value is precisely cancelled by the negative-energy sum. A test of the TRK sum rule using the spectra for higher values of angular momenta generated using B splines with $n=40$ and $k=7$ in a Coulomb potential with $Z=2$ is given in Table II. It is seen in the second column of the table that the cancellation between positive and negative terms is better than one part in 10^8 for all l from 0 to 9. By increasing the number of splines to 50 and the order to $k=9$, we can improve the cancellation to one part in 10^{10}. The deviation of the sum over positive-energy states from the non-

TABLE I. Eigenvalues of the symmetric generalized eigenvalue equation using the B-spline approximation to the radial Dirac equation with $\kappa=-1$ in a Coulomb potential with $Z=2$. Cavity radius $R=40$ a.u. First interior knot=0.002 a.u. In this example we use 40 B-splines with $k=7$.

State	B-spline negative energy $+mc^2$	B-spline positive energy $-mc^2$	Coulomb-field Dirac equation nl	$E_{nl}-mc^2$
1	−0.078 471 97	−2.000 106 51	1s	−2.000 106 51
2	−0.109 143 10	−0.500 033 30	2s	−0.500 033 29
3	−0.142 954 85	−0.222 234 07	3s	−0.222 234 06
4	−0.180 036 09	−0.125 006 46	4s	−0.125 005 41
5	−0.221 198 17	−0.079 983 39	5s	−0.080 002 90
6	−0.294 385 07	−0.053 800 99	6s	−0.055 557 28
7	−0.410 869 99	−0.027 408 78		
8	−0.434 354 48	0.006 542 98		
9	−0.646 069 74	0.054 643 23		
10	−1.013 370 89	0.100 681 88		
11	−1.637 309 78	0.299 878 95		
12	−2.715 450 51	0.409 558 14		
13	−4.614 618 75	1.248497 17		
14	−8.024 337 76	3.201 910 43		
15	−14.252 754 33	7.428 459 45		
16	−25.796 495 63	16.209 284 03		
17	−47.437 726 81	34.021 348 79		
18	−88.352 223 09	69.614 219 24		
19	−166.134 287 73	139.990 167 71		
20	−173.523 244 22	173.420 032 77		
21	−314.400 613 26	277.929 605 23		
22	−596.702 314 65	545.830 743 09		
23	−1130.836 317 38	1059.861 618 26		
24	−2127.138 566 52	2028.071 814 96		
25	−3938.569 289 68	3800.195 101 68		
26	−7106.585 370 09	6913.111 748 28		
27	−12 381.547 232 42	12 110.643 789 28		
28	−20 732.296 337 31	20 352.198 334 24		
29	−33 412.084 262 86	32 877.223 807 26		
30	−52 139.484 483 56	51 383.705 083 68		
31	−79 416.568 374 23	78 342.163 985 55		
32	−119 041.601 910 54	117 500.669 513 58		
33	−177 001.370 250 39	174 761.830 893 22		
34	−263 213.774 924 33	259 891.669 075 92		
35	−395 381.458 683 81	390 289.406 599 54		
36	−608 884.963 766 40	600 640.062 501 82		
37	−987 203.926 834 66	972 520.980 500 20		
38	−1 779 801.130 631 16	1 748 823.576 101 66		
39	−4 087 410.996 309 64	3 994 928.816 607 04		
40	−23 278 423.462 308 17	22 637 209.288 290 02		

TABLE II. Test of the relativistic TRK sum rule Eq. (26) for various l using a B-spline representation of the Coulomb-field Dirac equation confined to a cavity of radius $R=40$ a.u. We use 40 B-splines with $k=7$. The basis set for $\kappa=-1$ is the same as that used in Table I.

l	Sum over positive- and negative-energy states	Sum over positive-energy states only	Nonrelativistic limit $[(l+1)l+1]/2$
0	6.6×10^{-9}	0.499 74	0.5
1	6.8×10^{-9}	1.499 73	1.5
2	6.3×10^{-9}	3.497 33	3.5
3	6.3×10^{-9}	6.488 21	6.5
4	6.3×10^{-9}	10.466 37	10.5
5	6.4×10^{-9}	15.424 40	15.5
6	6.8×10^{-9}	21.353 69	21.5
7	6.6×10^{-9}	28.244 58	28.5
8	7.0×10^{-9}	36.086 54	36.5
9	7.7×10^{-9}	44.868 31	45.5

relativistic limit shown in column 3 is a real relativistic effect, independent of the radius of the cavity.

Another test of the quality of the spectrum is the value of the dipole polarizability α_d, which is known exactly for an electron in a Coulomb field in the nonrelativistic limit, and analyically to order $(\alpha Z)^2$ in the relativistic case; for $Z=2$, the $n=50$, $k=9$ spline routine gives

$$\alpha_d = 0.281\,187\,877\cdots a_0^3 , \tag{28}$$

compared to Kaneko's analytic result[18]

$$\alpha_d = [\tfrac{9}{2} - \tfrac{14}{3}(\alpha Z)^2 + \cdots]Z^{-4}a_0^3 = 0.281\,187\,873\cdots a_0^3 . \tag{29}$$

Other tests of the spectrum include energy weighted sum rules such as the second energy weighted sum rule:[9]

$$S_2 = \tfrac{2}{9}\sum_n \omega_{n0}^2 |\langle \kappa=-1, n=0 | r | \kappa=1, n\rangle|^2 + \tfrac{4}{9}\sum_n \omega_{n0}^2 |\langle \kappa=-1, n=0 | r | \kappa=-2, n\rangle|^2 = \alpha^{-2} . \tag{30}$$

We obtain the value α^{-2} to an accuracy of one part in 10^8 using the $n=40$, $k=7$, $Z=2$, Coulomb-field spline spectrum, and to one part in 10^{10} using a spectrum with $n=50$ and $k=9$.

As a direct application of the B-spline basis to a problem arising in relativistic many-body perturbation theory we have considered the calculation of the second-order corrections to the energy of helium starting from a Dirac Coulomb-field approximation.[19] The expression for the second-order energy, which contains a relativistic pair function implicitly, is

$$E^{(2)} = \sum_l \left[\frac{l}{(2l+1)^3}\sum_{n,m}\frac{R_l(n\kappa,m\kappa,1s,1s)^2}{(2\epsilon_{1s}-\epsilon_{n\kappa}-\epsilon_{m\kappa})}\bigg|_{\kappa=l} + \frac{l+1}{(2l+1)^3}\sum_{n,m}\frac{R_l(n\kappa,m\kappa,1s,1s)^2}{(2\epsilon_{1s}-\epsilon_{n\kappa}-\epsilon_{m\kappa})}\bigg|_{\kappa=-l-1}\right] . \tag{31}$$

The quantities $R_l(a,b,c,d)$ are Slater integrals, defined by

$$R_l(a,b,c,d) = \int dr \int dr' \frac{r_<^l}{r_>^{l+1}}[P_a(r)P_c(r)+Q_a(r)Q_c(r)] \times [P_b(r')P_d(r')+Q_b(r')Q_d(r')] . \tag{32}$$

In Eq. (31) the sums over n and m are restricted to the positive-energy states. The nonrelativistic sums corresponding to Eq. (31) have been carried out to high accuracy[20] giving $E_{nr}^{(2)} = -0.157\,666\,43\cdots$. Using our B-spline basis, with $n=50$ and $k=9$ for helium, we find

$$E^{(2)} = -0.157\,681\,47 = -0.157\,666\,43 - 0.071(\alpha Z)^2 . \tag{33}$$

The corresponding second-order Breit interaction (one Breit plus one Coulomb) gives the result

$$B^{(2)} = -0.563(\alpha Z)^2 . \tag{34}$$

We can compare the total relativistic corrections to the second-order energy,

$$\Delta E_{\rm rel}^{(2)} = -(0.071+0.563)(\alpha Z^2) = -0.634(\alpha Z)^2 , \tag{35}$$

with values obtained by Drake[21] who calculated the leading coefficients in a $1/Z$ expansion of the relativistic interaction using correlated nonrelativistic basis sets

$$\Delta E_{\rm rel}^{(2)} = -(0.070+0.565)(\alpha Z)^2 = -0.635(\alpha Z)^2 . \tag{36}$$

It is seen that the B splines provide a basis of high enough quality to permit the study of the small relativistic effects in an atom as light as helium.

A further application of the B-spline approximation is given in Table III where the low-lying positive-energy levels of the thallium atom ($Z=81$) determined by solving the Dirac equation in a Tietz potential are compared with the lowest positive-energy eigenvalues obtained using the B-spline approximation with $n=50$ and $k=9$. The cavity radius was chosen to be $R=50$ a.u. For a

TABLE III. Comparison of energies (a.u.) of low-lying positive-energy states in *Tl* ($Z=81$) determined by numerical integration of the Dirac equation in a modified Tietz potential (Ref. 25),

$$V(r)=-\frac{\alpha}{r}\left[1+\frac{Z-1}{(1+tr)^2}e^{-\gamma r}\right],$$

with the corresponding states determined using the *B*-spline approximation with $n=50$, $k=9$, and $R=50$ a.u. Tietz parameters: $t=2.3537$, $\gamma=0.3895$. Nuclear charge distribution: uniform $R_{\mathrm{RMS}}=5.483$ fm.

n	Tietz	*B*-spline[a]	Tietz	*B*-spline	Tietz	*B*-spline
	$s_{1/2}$		$p_{1/2}$		$p_{3/2}$	
1	−3244.088 041	−3244.088 175				
2	−600.337 909	−600.337 931	−587.968 349	−587.968 347	−504.453 288	−504.453 288
3	−144.284 503	−144.284 508	−136.371 558	−136.371 558	−117.163 505	−117.163 505
4	−31.769 938	−31.769 939	−27.753 537	−27.753 538	−23.123 674	−23.123 674
5	−4.877 629	−4.877 630	−3.454 693	−3.454 693	−2.661 872	−2.661 872
6	−0.453 947	−0.453 947	−0.224 542	−0.224 542	−0.183 199	−0.183 199
7	−0.101 906	−0.101 906	−0.069 323	−0.069 323	−0.063 913	−0.063 913
	$d_{3/2}$		$d_{5/2}$		$f_{5/2}$	
3	−101.791 588	−101.791 588	−97.296 059	−97.296 059		
4	−15.808 594	−15.808 594	−14.872 298	−14.872 298	−4.517 716	−4.517 716
5	−0.648 139	−0.648 139	−0.565 324	−0.565 324	−0.031 418	−0.031 414
6	−0.058 334	−0.058 334	−0.057 804	−0.057 804	−0.020 122	−0.019 458
7	−0.032 425	−0.032 415	−0.032 166	−0.032 155	−0.013 971	−0.007 897
	$f_{7/2}$		$g_{7/2,9/2}$		$h_{9/2,11/2}$	
4	−4.301 590	−4.301 590				
5	−0.031 418	−0.031 414	−0.020 005	−0.019 781		
6	−0.020 122	−0.019 458	−0.013 894	−0.010 178	−0.013 889	−0.012 427
7	−0.013 970	−0.007 897	−0.010 208	0.003 559	−0.010 204	−0.001 413

[a]The first nonzero knot on the radial grid, t_{10}, is chosen to be 0.0001 a.u. for *s* and *p* states, 0.001 a.u. for *d* and *f* states, and 0.01 a.u. for *g* and *h* states.

strong Coulomb potential the effects of nuclear finite size are important, especially for *s* and *p* states. We include finite nuclear size in this example assuming a uniform nuclear charge distribution. The first nonzero knot for *s* and *p* states is chosen to be at 0.0001 a.u. in order to force the first k *B* splines to overlap the nucleus. For states of higher angular momentum the first knot was moved further out in order to improve the knot distribution over the cavity. Small differences seen in the table for the energies of the $s_{1/2}$ and $p_{1/2}$ states could be reduced by choosing a denser grid near the origin. The differences seen for the very weakly bound states of high angular momentum illustrate the effects of the finite cavity radius.

While it is useful to have a basis for the Dirac equation in a central potential that is of high quality, it is even more useful to have a finite basis for the Dirac-Hartree-Fock (DHF) equations.[22] Finite-basis-set techniques have been used previously to obtain DHF core orbitals by Kim[23] and more recently by Goldman and Dalgarno.[24] Our goal is somewhat different; we are interested in obtaining a "complete" set of DHF basis orbitals that can be used to carry out the intermediate-state sums occurring in higher-order perturbation theory.

In our applications we are particularly interested in solving the $V(N-1)$ DHF equations for alkali-metal atoms and other atoms having one electron outside a closed core. For the core electrons the $V(N-1)$ DHF equations may be written

$$(H_\kappa+V_{\mathrm{HF}})\varphi_a(r)=\epsilon_a\varphi_a(r)\ . \tag{37}$$

where $\varphi_a(r)$ is a two-component radial wave function for orbital a, and where $H_\kappa+V_{\mathrm{HF}}$ is a 2×2 radial Hamiltonian operator, such as that written out on the left-hand side of Eq. (6), but with the core Hartree-Fock potential added to the nuclear potential $V(r)$. The Hartree-Fock potential can be included without difficulty in the action functional S of Eq. (7). The matrix A in Eq. (16) becomes considerably more complex with the Hartree-Fock potential, owing to the presence of nonlocal exchange terms, but the form of the eigenvalue equation remains unchanged.

The procedure used in the DHF case is to solve the DHF equations using a point-by-point numerical integration scheme, then to use the core DHF orbitals to calculate the potential V_{HF} in the action functional S. Once the matrix A has been constructed, the eigenvalue equation is solved to find the entire DHF spectrum for a given κ. The radius of the cavity is chosen large enough that the low-lying positive-energy states of a given angular symmetry agree closely with the input DHF states of the same angular symmetry. In addition to the core

TABLE IV. Comparison of the DHF eigenvalues for some low-lying bound states of cesium, $Z=55$, determined from the B-spline approximation using $n=50$, $k=9$, $R=50.0$ a.u., with eigenvalues calculated using standard finite-difference methods. Nuclear Fermi charge distribution parameters: $c_{\rm nuc}=5.674$ fm, $t_{\rm nuc}=2.3$ fm.

n	DHF	B-spline	DHF	B-spline	DHF	B-spline
	$s_{1/2}$		$p_{1/2}$		$p_{3/2}$	
1	−1330.118 917	−1330.118 530				
2	−212.564 461	−212.564 413	−199.429 431	−199.429 429	−186.436 550	−186.436 550
3	−45.969 741	−45.969 731	−40.448 293	−40.448 293	−37.894 301	−37.894 301
4	−9.512 822	−9.512 820	−7.446 284	−7.446 284	−6.921 001	−6.921 001
5	−1.489 806	−1.489 806	−0.907 898	−0.907 898	−0.840 340	−0.840 340
6	−0.127 368	−0.127 368	−0.085 616	−0.085 616	−0.083 785	−0.083 785
7	−0.055 187	−0.055 187	−0.042 021	−0.042 021	−0.041 368	−0.041 367
	$d_{3/2}$		$d_{5/2}$		$f_{5/2}$	
3	−28.309 496	−28.309 496	−27.775 153	−27.775 153		
4	−3.485 618	−3.485 619	−3.396 901	−3.396 901	−0.031 274	−0.031 269
5	−0.064 420	−0.064 420	−0.064 530	−0.064 530	−0.020 019	−0.019 325
6	−0.036 087	−0.036 085	−0.036 090	−0.036 088	−0.013 903	−0.007 673
7	−0.022 622	−0.022 123	−0.022 613	−0.022 111		
	$f_{7/2}$		$g_{7/2}$		$g_{9/2}$	
4	−0.031 273	−0.031 270				
5	−0.020 020	−0.019 326	−0.020 000	−0.019 776	−0.020 000	−0.019 776
6	−0.013 903	−0.007 675	−0.013 889	−0.010 634	−0.013 889	−0.010 634

states, the B-spline spectrum contains approximations for the remaining positive- and negative-energy terms in the DHF spectrum. One test of how well the parameters defining the spline approximation are chosen is how well the input and output core states agree with each other. Comparisons can be made between valence states calculated using the B-spline approximation and valence DHF functions obtained by direct numerical solution of the DHF differential equations to see whether or not the cavity radius has been chosen properly. Such a comparison is given in Table IV, where the energies of occupied states and low-lying valance states of cesium, calculated using a B-spline approximation with $n=50$, $k=9$, and $R=50$ a.u., are given together with energies obtained by solving the DHF equations using finite-difference methods. The small differences seen in the innermost s- and p-state energies are not caused by the finite cavity radius; these differences can be reduced by choosing a denser grid near $r=0$. The differences seen in the table for the weakly bound d, f, and g states are due to the finite cavity radius and can be reduced by choosing a larger cavity radius. To generate 100 terms in each of the 19 DHF B-spline spectra for cesium corresponding to $\kappa=-1, 1, -2, \cdots, -10$, required a total of about 10 min on a CRAY XMP/48 computer.

In the above paragraphs we have given a detailed theoretical description of how B splines can be used to provide practically useful sets of basis functions for the Dirac equation, and to show a few of the tests that have been made to determine the quality of the resulting basis. Applications of the B-spline basis sets to calculate second-order energies and third-order hyperfine constants and transition amplitudes for alkali-metal atoms have been carried out and reported in Ref. 22. Further applications to calculate third-order energies and to determine correlation corrections to parity nonconserving amplitudes are underway.

ACKNOWLEDGMENTS

This work was supported in part by National Science Foundation Grants Nos. PHY-86-08101 and PHY-85-03417. One of the authors (W.R.J.) owes thanks to A. Dalgarno for hospitality at the Harvard-Smithsonian Center for Astrophysics (Cambridge, MA), where some of the work was carried out. A debt of gratitude is also owed to C. Bottcher for an introduction to B-spline methods.

[1]H. P. Kelly, Phys. Rev. **131**, 684 (1963).
[2]M. Vajed-Samii, S. N. Ray, T. P. Das, and J. Andrissen, Phys. Rev. A **20**, 1787 (1970); V. A. Dzuba, V. V. Flambaum, and O. P. Sushkov, J. Phys. B **16**, 715 (1983).
[3]R. M. Sternheimer, Phys. Rev. **80**, 102 (1950).
[4]A. Dalgarno and J. T. Lewis, Proc. R. Soc. London, Ser. A **233**, 70 (1955).
[5]V. McKoy and N. W. Winter, J. Chem. Phys. **48**, 5514 (1968).
[6]J. I. Musher and J. M. Schulman, Phys. Rev. **173**, 93 (1968).
[7]I. Lindgren and J. Morrison, *Atomic Many-Body Theory,* 2nd ed. (Springer, Berlin, 1986), p. 326.
[8]E. Lindroth, Phys. Rev. A **37**, 316 (1988).
[9]G. W. F. Drake and S. P. Goldman, Phys. Rev. A **23**, 2093 (1981).
[10]I. P. Grant, Phys. Rev. A **25**, 1220 (1982).
[11]W. Kutzelnigg, Int. J. Quantum Chem. **25**, 107 (1974).

[12]A. Chodos, R. L. Jaffe, K. Johnson, C. B. Thorn, and V. W. Weisskopf, Phys. Rev. D **9**, 3471 (1974).
[13]J. J. Sakurai, *Advanced Quantum Mechanics* (Addison-Wesley, Reading, MA, 1967), p. 120.
[14]C. deBoor, *A Practical Guide to Splines* (Springer, New York, 1978).
[15]C. Bottcher and M. R. Strayer, Ann. Phys. (N.Y.) **175**, 64 (1987).
[16]C. W. A. Fletcher, *Computational Galerkin Methods* (Springer, New York, 1984).
[17]B. S. Garbow, J. M. Boyle, J. J. Dongarra, and C. B. Moler, *Matrix Eigensystem Routines—EISPACK Guide Extension* (Springer, Berlin, 1977), p. 250.
[18]S. Kaneko, J. Phys. B **10**, 3347 (1977).
[19]W. R. Johnson and J. Sapirstein, Phys. Rev. Lett. **57**, 1126 (1986).
[20]J. D. Baker, D. E. Freund, R. N. Hill, and J. D. Morgan, Phys. Rev. A (to be published).
[21]G. W. F. Drake, Phys. Rev. A **19**, 1387 (1979); (private communication).
[22]W. R. Johnson, M. Idrees, and J. Sapirstein, Phys. Rev. A **35**, 3218 (1987).
[23]Y.-K. Kim, Phys. Rev. **154**, 17 (1967).
[24]S. P. Goldman and A. Dalgarno, Phys. Rev. Lett. **57**, 408 (1986).
[25]T. Tietz, J. Chem. Phys. **22**, 2094 (1954); W. R. Johnson, D. S. Guo, M. Idrees, and J. Sapirstein, Phys. Rev. A **34**, 1057 (1986).